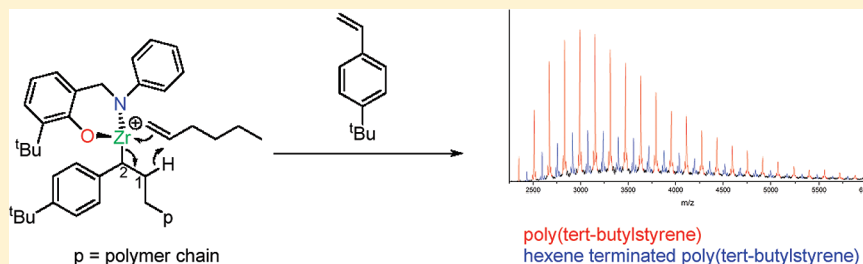


## Zirconium-Catalyzed Polymerization of a Styrene: Catalyst Reactivation Mechanisms Using Alkenes and Dihydrogen

Giles W. Theaker,<sup>†,‡</sup> Colin Morton,<sup>‡</sup> and Peter Scott<sup>\*,†</sup><sup>†</sup>Department of Chemistry, University of Warwick, Gibbet Hill Road, Coventry, UK CV4 7AL<sup>‡</sup>Infinium UK Ltd., Milton Hill, Abingdon, UK OX13 6BB

S Supporting Information

## ABSTRACT:



Zirconium salicylaldiminates in the presence of  $\text{Al}^i\text{Bu}_3/[\text{Ph}_3\text{C}][\text{B}(\text{C}_6\text{F}_5)_4]$  are inactive for the homopolymerization of *p*-tert-butylstyrene (TBS), but the addition of hexene leads to a highly active system. Analysis of the polymers by NMR and MALDI indicates surprisingly that most of the product chains contain no hexene, while some contain a single hexene unit. Addition of dihydrogen also leads to the production of poly(TBS) without substantial reduction in molecular weight and with main-chain end-group unsaturation. These and other observations lead us to two related mechanisms for the hexene- and dihydrogen-promoted reactions. Synthetic and catalytic studies indicate that the active species is not a typical bis(salicylaldiminato) compound but an amido/alkoxido system. An authentic compound of this class is highly active for the TBS polymerization even in the absence of added aluminum alkyl.

## INTRODUCTION

The controlled synthesis of polystyrene (PS) has been achieved using a number of polymerization mechanisms,<sup>1,2</sup> leading to various tacticities, regiochemistries, and molecular weights. Examples include the production of atactic polystyrene (aPS) on an industrial scale by radical polymerization methods and the formation of syndio- and isotactic polystyrene (sPS and iPS) via cationic transition-metal-mediated coordination polymerization. The latter area is dominated by titanium catalysts which give excellent conversion, activity, and stereocontrol for either sPS or iPS. Indeed, the first synthesis of sPS<sup>3</sup> by Ishihara<sup>4</sup> used  $\text{CpTiCl}_3$  activated with methylaluminoxane (MAO), and this remains a benchmark system today.

Zirconium-based systems have been less successful. Several studies have looked at styrene polymerizations with simple zirconium complexes such as  $\text{Zr}(\text{CH}_2\text{Ph})_4$ ,<sup>5</sup>  $\text{ZrCl}_4$ ,<sup>6</sup> and  $\text{ZrCl}_4 \cdot \text{THF}_2$ ,<sup>7</sup> alongside metallocenes ( $\text{Cp}_2\text{ZrCl}_2$ ),<sup>8</sup> half-sandwich complexes ( $\text{CpZrCl}_3$ ),<sup>8</sup> *ansa*-zirconocenes,<sup>9,10</sup> and post-metallocenes such as “OSSO”-based systems.<sup>11</sup> While production of both sPS and iPS has been achieved,<sup>8</sup> the activities displayed by these systems are extremely low compared with their titanium equivalents. The larger radius and lower electrophilicity of zirconium have been suggested as the reasons behind this difference in behavior (vide infra).

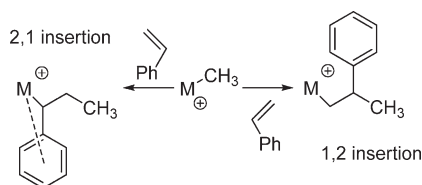
Early copolymerizations of styrene and ethene with  $\text{CpTiCl}_3$  produced homopolymers of both monomers as mixtures with the ES copolymer.<sup>12</sup> This implies the presence of multiple catalytic species in the reaction mixture. Studies conducted into the nature of the active species in titanium-mediated styrene polymerizations have implicated  $\text{Ti}^{\text{III}}$  in the homopolymerization of styrene and  $\text{Ti}^{\text{IV}}$  in the homopolymerization of ethene, though there is evidence that the system may not be this simple.<sup>13</sup> Regardless,  $\text{Ti}^{\text{IV}}$  species such as  $\text{CpTiCl}_3$  are readily reduced by the aluminum alkyls such as  $\text{Al}^i\text{Bu}_3$  or those present in MAO.<sup>14</sup>  $\text{Ti}^{\text{III}}$  species such as  $(\text{CpTiOMe})_2\mu\text{-(OMe)}_2$  have been shown to have activity for sPS production in excess of that of their  $\text{Ti}^{\text{IV}}$  analogues,<sup>8</sup> while EPR studies have shown that increased  $[\text{Ti}^{\text{III}}]$  corresponds with higher activity for PS production.<sup>15–17</sup> Overall then,  $\text{Ti}^{\text{III}}$  is implicated strongly in PS catalysis, and this is perhaps a good reason why this metal is far more successful than ( $d^0$ ) zirconium.

Ethene/styrene (ES) copolymers are of great interest both commercially<sup>18</sup> and academically, but as noted above, PS producing catalysts are less useful for ES copolymerization, as

Received: December 13, 2010

Revised: January 24, 2011

Published: February 14, 2011

Scheme 1. Insertions of Styrene in a Metal–Alkyl<sup>a</sup>

<sup>a</sup> A 2,1 insertion leads to the benzylic “dormant state”.

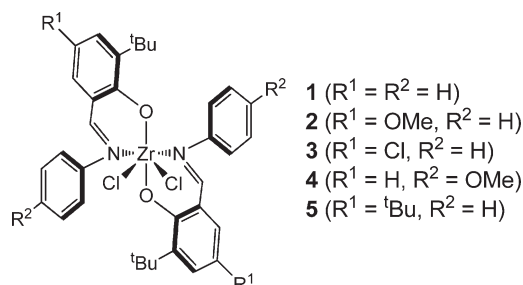


Figure 1. Bis(salicylaldimine)zirconium precatalysts 1–5.

homopolymer blends are a likely result. With non-PS producing catalysts, production of P(E/S) is hampered due to the adverse effects of styrene on the catalyst involved. For example, the classic metallocene  $\text{Cp}_2\text{ZrCl}_2/\text{MAO}$  system is essentially inactive for styrene homopolymerization, and correspondingly addition of styrene comonomer to an ethene polymerization results in a dramatic decrease in activity despite there being only minor incorporation of styrene into the polymer formed.<sup>19</sup> The constrained geometry catalyst (CGC)  $[(\text{Me}_2\text{SiCp}^*\text{N}^t\text{Bu})\text{TiCl}_2]/\text{MAO}$  also suffers from addition of styrene, but less so than for  $\text{Cp}_2\text{ZrCl}_2$ . Copolymers with up to 35 mol % styrene have been recorded when using this catalyst system in the presence of extremely high styrene concentrations,<sup>20,21</sup> while recent modifications to the Cp ring resulted impressively in a 31 mol % styrene copolymer under more conventional conditions.<sup>22</sup>

Both experimental and theoretical approaches to the styrene problem have indicated that this adverse effect is the result of a 2,1 insertion of styrene into a growing polymer chain. The resulting benzylic species is resistant to further monomer insertion as a result of coordination of the arene to the cationic metal center and is regarded as a “dormant state” (Scheme 1).<sup>20</sup> The contrast with PS producing catalysts such as  $\text{CpTiCl}_3$  is interesting, however; here, 2,1 insertion of styrene is the norm, and high activity is evident.

The use of substituted styrene monomers can have an effect on the rate or insertion mode of the monomer into the growing polymer chain.<sup>23,24</sup> Oliva and co-workers have shown in a model system that the ratio of styrenic 1,2 to 2,1 insertions varies with the electronic effect of *para*-substitution.<sup>25</sup> We have exploited this effect and shown that *tert*-butylstyrene (TBS) readily forms ethene-*co*-TBS polymers with up to 44 mol % comonomer at low TBS concentrations using Ti CGC.<sup>26</sup> Furthermore, while the zirconium salicylaldimine systems (Figure 1) developed by Fujita<sup>27–29</sup> and Coates<sup>30–32</sup> are inactive in the presence of styrene,<sup>33</sup> precatalysts 1–3 in combination with MAO produce unimodal ethene-*co*-TBS polymers with very high activity and long catalyst life.<sup>34</sup>

Here we will describe our discovery of very high and unexpected TBS homopolymerization activity by zirconium

salicylaldimine precatalysts when activated by tri-*i*-butylaluminum ( $\text{Al}^i\text{Bu}_3$ ) and the trityl borate salt  $[\text{Ph}_3\text{C}][\text{B}(\text{C}_6\text{F}_5)_4]$  along with an investigation of the mechanism of such polymerization.

## EXPERIMENTAL SECTION

**General Considerations.** Where necessary, the work detailed below was carried out under an inert atmosphere of argon, using standard Schlenk techniques. All glassware, cannula, syringes, etc., were dried at 150 °C for 24 h prior to use. Solvents were dried by reflux over an appropriate drying agent (pentane: NaK alloy; THF: potassium; toluene: sodium; dichloromethane:  $\text{CaH}_2$ ) for 3 days prior to distillation and then freeze–thaw–degassed three times before use. Deuterated solvents for NMR were refluxed over potassium (benzene, toluene, tetrahydrofuran) or calcium hydride (pyridine, dichloromethane) for 3 days before being vacuum transferred to a fresh ampule and stored under argon. Unless stated otherwise, reagents were used as purchased. Metal complexes and pyrophoric reagents were stored in an MBraun glovebox at <0.5 ppm of  $\text{O}_2$ .

NMR spectra of precursors and complexes were recorded on either Bruker DPX-400 or DRX-500 spectrometers. Residual protio-solvent was used as an internal reference.<sup>35</sup>  $^{13}\text{C}$  NMR spectra of ethene/styrenic copolymers were recorded on a Bruker DPX at 400 MHz in 1,1,2,2-tetrachloroethane (10 000 scans, 4 s relaxation time, 90 °C), ensuring that the sample was fully dissolved.  $^{13}\text{C}$  NMR of P(TBS) was carried out on a Bruker DPX at 400 MHz in  $\text{CDCl}_3$  at room temperature. Mass spectrometry of non-air-sensitive compounds was carried out on a Bruker Esquire2000 ESI spectrometer. Air-sensitive compounds were analyzed on a Bruker Ultraflex II TOF/TOF using 9-nitroanthracene as the organic matrix. Calibration was achieved using a mixture of  $\text{C}_{60}$ ,  $\text{C}_{78}$ , and  $\text{C}_{90}$ . P(TBS) samples were analyzed on the above machine using either DCTB or 9-nitroanthracene as the organic matrix and 0.1% AgTFA. Calibration was achieved using poly(ethylene glycol) (PEG) with 2–5000  $M_n$ . Elemental analysis was performed by Warwick Analytical Services or Medac Ltd.

*tert*-Butylstyrene, styrene, all  $\alpha$ -olefins, silanes, and additional monomers were purchased from Aldrich and stirred over  $\text{CaH}_2$  for 48 h and then vacuum-distilled and stored under argon. Methylaluminoxane (10% (w/v) in toluene) was purchased from Witco.

High-temperature GPC was run at RAPRA, utilizing a Polymer Laboratories GPC220 with a PLgel guard column and two 30 cm Mixed Bed B columns in 1,2,4-trichlorobenzene at 160 °C. Room temperature GPC analysis was carried out on a Varian 390LC with PLgel mixed D column in THF/2% triethylamine. Thermal analyses were carried out on a Perkin-Elmer PC7 series system. Sample masses in each case were ca. 3 mg, and the samples were purged with dinitrogen.

**Crystallography.** Crystals were coated in inert oil prior to transfer to a cold nitrogen gas stream on an Oxford Diffraction Gemini four-circle system with Ruby CCD area detector and held at 100(2) K with the Oxford Cryosystem Cryostream Cobra. The structure was solved by direct methods (SHELXTL) with additional light atoms found by Fourier methods. Hydrogen atoms were added at calculated positions and refined using a riding model with freely rotating methyl groups.

**General Procedure for Polymerizations with Monitored Gas Uptake.** Polymerizations were carried out in a jacketed 500 mL vessel equipped with a Pt thermocouple and buret system for the monitoring of gas delivery at a fixed pressure. Toluene, comonomer, and MAO (1000 equiv) were charged into a measuring ampule and transferred by cannula into the jacketed vessel. The argon atmosphere was replaced by ethene at 1.2 bar. The vessel was heated by a thermostatic recirculator unit. The precatalyst was dissolved in toluene no more than 5 min prior to use and injected into the jacketed vessel to begin the polymerization. Reactions were terminated by addition of methanol (5 mL), and the polymer was precipitated by pouring into

MeOH/5% HCl<sub>(aq)</sub>. The sample was filtered on a glass sinter and dried in a vacuum oven at 70 °C for 16 h.

**General Procedure for Schlenk-Based Polymerizations.** A Schlenk vessel equipped with stirrer bar was charged with the required comonomers and toluene under argon. A toluene solution of first [Ph<sub>3</sub>C][B(C<sub>6</sub>F<sub>5</sub>)<sub>4</sub>] and then triisobutylaluminum (Al<sup>i</sup>Bu<sub>3</sub>) was added via cannula. The reaction mixture was stirred and warmed to reaction temperature using an aluminum heating block. The precatalyst was dissolved in toluene no more than 5 min prior to use and was added via syringe. If required, the Schlenk vessel was carefully evacuated and refilled twice with H<sub>2</sub>(g) at 1.1 bar. Reactions were terminated by addition of methanol (5 mL), and the polymer was precipitated by pouring into MeOH/5% HCl<sub>(aq)</sub>. The sample was filtered on a glass sinter and dried in a vacuum oven at 70 °C for 16 h.

**Synthesis.** Precatalysts **1**–**3** and **5**, proligands HL<sup>1–3,5,6</sup> and precursors were synthesized as previously reported,<sup>34,36</sup> as was zirconium tetrabenzyl.<sup>37</sup> Ligands HL<sup>4</sup> and H<sub>2</sub>L<sup>7,38</sup> and precatalysts **4**, **6**,<sup>36</sup> and **7**<sup>38</sup> were synthesized as reported below.

**HL<sup>4</sup>.** 2-Hydroxy-3-*tert*-butylbenzaldehyde (2.02 g, 11.35 mmol) and anisidine (2.09 g, 17.0 mmol) were dissolved in methanol (40 mL) and heated to reflux for 12 h. The solution was cooled to 4 °C, and the pale orange powder precipitate was collected by vacuum filtration (1.15 g, 35%). <sup>1</sup>H NMR (400 MHz, CDCl<sub>3</sub>): δ 13.97 (1H, s, OH), 8.59 (1H, s, CHN), 7.30 (1H, s, Ar), 7.28 (3H, m, Ar), 7.02 (1H, d, <sup>3</sup>J = 2 Hz, Ar), 6.97 (1H, s, Ar), 6.95 (1H, s, Ar), 3.86 (3H, s, OMe), 1.49 (9H, s, <sup>t</sup>Bu). <sup>13</sup>C NMR (100 MHz, CDCl<sub>3</sub>): δ 161.3 (CN), 158.7, 141.4, 137.6 (Ar-q), 130.9 (Ar), 130.6 (Ar-q), 130.0 (Ar), 122.27 (Ar), 119.0 (Ar-q), 114.6 (Ar), 55.5 (OMe), 34.9 (<sup>t</sup>Bu q), 29.4 (<sup>t</sup>Bu). Anal. Calcd C: 76.29, H: 7.47, N: 4.94. Found C: 76.29, H: 7.31, N: 4.49. MS (CI) *m/z*: 284.4 [M + H]<sup>+</sup>.

**L<sup>4</sup>ZrCl<sub>2</sub> (4).** HL<sup>4</sup> (0.90 g, 3.17 mmol) and NaH (excess) were charged into a Schlenk vessel and cooled to –78 °C. Dry THF (40 mL) was added, and the solution was stirred at ambient temperature for 18 h. The resulting solution was filtered via cannula directly onto ZrCl<sub>4</sub>·THF<sub>2</sub> (0.54 g, 1.42 mmol) in dry THF (20 mL) at –78 °C. After stirring overnight, the solvent was removed in vacuo, yielding a yellow solid. This was further purified via sublimation (5 × 10<sup>–6</sup> mbar, 260 °C) to give 0.7 g, 68%. Crystals suitable for X-ray diffraction were obtained from DCM at –30 °C. <sup>1</sup>H NMR (400 MHz, –60 °C, CD<sub>2</sub>Cl<sub>2</sub>): δ 8.14 (2H, s, CHN), 7.46 (2H, d, <sup>3</sup>J = 8 Hz, Ar), 7.14 (2H, d, <sup>3</sup>J = 8 Hz, Ar), 7.00 (4H, d, <sup>3</sup>J = 9 Hz, Ar), 6.86 (2H, t, <sup>3</sup>J = 8 Hz, Ar), 6.59 (4H, d, <sup>3</sup>J = 9 Hz, Ar), 3.65 (6H, s, OMe), 1.40 (18H, s, <sup>t</sup>Bu). <sup>13</sup>C NMR (100 MHz, Pyr): δ 137.4, 136.0, 135.8, 126.4, 116.0 (Ar), 57.11 (OMe), 36.8 (<sup>t</sup>Bu q), 31.6 (<sup>t</sup>Bu). Solubility of this complex is poor and quaternary aromatic peaks were not visible. Anal. Calcd for C<sub>36</sub>H<sub>40</sub>Cl<sub>2</sub>N<sub>2</sub>O<sub>4</sub>Zr: 59.49, H: 5.55, N: 3.85. Found C: 58.68, H: 5.39, N: 3.52. MS (MALDI) *m/z*: 689.1 [M – Cl]<sup>+</sup>.

**L<sup>6</sup>ZrCl<sub>2</sub> (6).** A Schlenk vessel equipped with stirrer bar was charged with HL<sup>6</sup> (0.40 g, 1.61 mmol) and NaH (0.077 g, 3.24 mmol) and cooled to –78 °C. Dry THF (30 mL) was added, and the solution was allowed to warm to room temperature with stirring. After 4 h, stirring was stopped and the precipitate allowed to settle. The solution

was transferred via filter cannula directly to a Schlenk vessel charged with ZrCl<sub>4</sub>·THF<sub>2</sub> (0.31 g, 0.81 mmol) and cooled to –78 °C. After stirring overnight, the solvent was removed in vacuo. The residue was dissolved in hot toluene, filtered, and allowed to cool to room temperature. The resulting precipitate was removed by filtration and washed in cold pentane, to yield an off white solid (220 mg, 38%). <sup>1</sup>H NMR (400 MHz, CD<sub>2</sub>Cl<sub>2</sub>): δ 7.26 (4H, s, Ar), 7.15 (1.5H, m, toluene Ar), 4.29 (2H, d, <sup>2</sup>J = 8.5 Hz, COCH<sub>2</sub>), 3.82 (6H, s, OCH<sub>3</sub>), 2.36 (1.5H, s, toluene CH<sub>3</sub>), 1.59 (6H, s, CH<sub>3</sub>), 1.57 (18H, s, <sup>t</sup>Bu), 1.20 (6H, s, CH<sub>3</sub>). <sup>13</sup>C NMR (100 MHz, CD<sub>2</sub>Cl<sub>2</sub>): δ 169.2 (C=N), 157.0, 152.6, 141.8 (Ar q), 129.0, 128.5 (toluene), 123.0 (Ar), 115.6 (Ar q), 109.4 (Ar), 79.4 (CH<sub>2</sub>), 70.3 (CMe<sub>2</sub>), 56.0 (OCH<sub>3</sub>), 35.5 (<sup>t</sup>Bu q), 30.0 (CMe<sub>3</sub>), 29.0 (CH<sub>3</sub>), 26.5 (CH<sub>3</sub>), 21.5 (toluene). Anal. Calcd for C<sub>32</sub>H<sub>44</sub>Cl<sub>2</sub>N<sub>2</sub>O<sub>6</sub>Zr·<sup>1</sup>/<sub>2</sub>(C<sub>7</sub>H<sub>8</sub>) C: 56.04, H: 6.36, N: 3.68. Found C: 56.26, H: 6.43, N: 3.55. MS (MALDI) *m/z*: 714.05 [M]<sup>+</sup>, 679.09 [M – Cl]<sup>+</sup>.

**H<sub>2</sub>L<sup>7</sup>.** Proligand HL<sup>2</sup> (1.10 g, 3.88 mmol) was charged into a round-bottom flask and purged with argon for ca. 5 min. Dry THF (80 mL) was added, followed by LiAlH<sub>4</sub> (0.73 g, 19.4 mmol), and the solution was stirred for 1.5 h. Diethyl ether was added, and the solution was cooled to –78 °C. Ice was carefully added, and the solution was allowed to warm to ambient temperature, with stirring. Further diethyl ether (100 mL) and NaOH<sub>(aq)</sub> (1 M, 100 mL) were added; the organic layer was separated and washed with water and then dried over Na<sub>2</sub>SO<sub>4</sub>. The diethyl ether was removed in vacuo, and the residue was dissolved in methanol. The solution was cooled to –30 °C overnight, and the resulting white crystals were collected by filtration (0.795 g, 71%). <sup>1</sup>H NMR (400 MHz, CDCl<sub>3</sub>): δ 8.21 (1H, s, OH), 7.18 (2H, t, <sup>3</sup>J = 7 Hz, Ar), 6.85 (1H, t, <sup>3</sup>J = 7 Hz, Ar), 6.80 (1H, d, <sup>3</sup>J = 3 Hz, Ar), 6.79 (1H, s, NH), 6.51 (1H, d, <sup>3</sup>J = 3 Hz, Ar), 4.28 (2H, d, <sup>3</sup>J = 6 Hz, CH<sub>2</sub>N), 3.70 (3H, s, OMe), 1.33 (9H, s, <sup>t</sup>Bu). <sup>13</sup>C NMR (100 MHz, CDCl<sub>3</sub>): δ 152.3, 149.7, 147.2, 138.6 (Ar q), 129.4 (Ar), 123.5 (Ar q), 120.9, 116.1, 113.3, 111.1 (Ar), 55.7 (OMe), 49.6 (CH<sub>2</sub>), 35.0 (<sup>t</sup>Bu q), 29.5 (<sup>t</sup>Bu). Anal. Calcd C: 75.76, H: 8.12, N: 4.91. Found C: 75.80, H: 8.17, N: 4.82. MS (EI) *m/z*: 286.1 [M]<sup>+</sup>.

**L<sup>7</sup>ZrBn<sub>2</sub> (7).** H<sub>2</sub>L<sup>7</sup> (104.6 mg, 0.37 mmol) and ZrBn<sub>4</sub> (168.2 mg, 0.37 mmol) were charged into a Schlenk vessel under argon and then cooled to –78 °C. DCM (20 mL) was added, and the solution stirred for 1 h. The solvent was removed in vacuo, and the residue was washed with cold pentane. The resulting light yellow solid (165 mg, 80%) was stored at –30 °C under argon to avoid decomposition. <sup>1</sup>H NMR (400 MHz, CD<sub>2</sub>Cl<sub>2</sub>): δ 7.34 (2H, t, <sup>3</sup>J = 8 Hz, Ar), 7.26 (1H, d, <sup>3</sup>J = 7 Hz, Ar), 7.14 (2H, m, Ar), 7.06 (3H, m, Ar), 6.83 (2H, t, <sup>3</sup>J = 7 Hz, Ar), 6.66 (2H, m, Ar), 6.53 (3H, m, Ar), 6.34 (2H, m, Ar), 5.31 (1H, s, DCM), 4.56, 3.54 (1H, d, <sup>2</sup>J = 17 Hz, CH<sub>2</sub>N), 3.79 (3H, s, OCH<sub>3</sub>), 2.66, 2.31 (1H, d, <sup>2</sup>J = 11 Hz, CH<sub>2</sub>Ph), 1.75, 1.55 (1H, d, <sup>2</sup>J = 11 Hz, CH<sub>2</sub>Ph), 1.25 (9H, s, <sup>t</sup>Bu). <sup>13</sup>C NMR (100 MHz, CD<sub>2</sub>Cl<sub>2</sub>): δ 152.2, 151.8, 149.0, 140.1, 136.9, 135.4, 129.0 (Ar q), 130.3, 129.9, 128.8, 128.5, 127.6, 126.5, 126.0, 125.7, 125.2, 121.4, 112.1 (Ar), 67.5, 64.0 (CH<sub>2</sub>Ph), 55.5 (OCH<sub>3</sub>), 53.2 (DCM), 50.8 (CH<sub>2</sub>N), 34.5 (<sup>t</sup>Bu q), 28.9 (<sup>t</sup>Bu). Anal. Calcd for C<sub>32</sub>H<sub>35</sub>NO<sub>2</sub>Zr·<sup>1</sup>/<sub>2</sub>(CH<sub>2</sub>Cl<sub>2</sub>) C: 65.87, H: 6.11, N: 2.37. Found C: 65.84, H: 6.15, N: 2.37. MS (MALDI) *m/z*: 538.63 [M – Me]<sup>+</sup>.

**Table 1. Initial Polymerization Results<sup>a</sup>**

run	cat.	cat. (mol)/10 <sup>–6</sup>	monomer system	yield (g)	mass prod <sup>b</sup>	TBS % conv	PDI	T <sub>M</sub> (°C)
1	1	9.00	E/TBS	1.8	200.0	n/d		96.5, 125.7
2	2	7.02	E/TBS	12.0	1710.2	40	66	91.0, 124.4
3	3	8.43	E/TBS	1.7	201.7	n/d		109.1, 117.1
4	2	6.88	E/TBS	4.3	3750.5	41		112.7, 119.3
5	2	8.12	E/St	0.4	49.3	n/d		
6	2	4.54	TBS	0.1	22.0	n/d		

<sup>a</sup> Conditions: [Ph<sub>3</sub>C][B(C<sub>6</sub>F<sub>5</sub>)<sub>4</sub>] = 1.1 equiv to Zr; Al<sup>i</sup>Bu<sub>3</sub> = 100 equiv to Zr; ethene at 1.2 bar; [TBS] = 0.07 M; volume = 100 mL (runs 1–5) or 50 mL (run 6); run time = 60 min (except run 44, 10 min); T = 40 °C. <sup>b</sup> In kg-polymer/(mol-catalyst h).



## RESULTS AND DISCUSSION

**Ethene/*tert*-Butylstyrene Copolymerizations.** We have previously shown that salicylaldehyde catalysts **1–3** on activation with MAO cleanly gave E/TBS copolymers.<sup>34</sup> In contrast, on activation of the same precatalysts with  $\text{Al}^i\text{Bu}_3/[\text{Ph}_3\text{C}][\text{B}(\text{C}_6\text{F}_5)_4]$  (Table 1 runs 1–4) led to production of mixtures of PE and P(TBS) (vide infra).

Catalyst **2** (run 2) was substantially more active and stable than catalysts **1** and **3** (runs 1 and 3), giving continuous ethene uptake over a 1 h period (Figure 2). Fractionation of the products by Soxhlet extraction into pentane failed to separate the components sufficiently, and GPC analysis returned traces with broad, multimodal distributions. The observation of two distinct melting points for sample 4 is consistent with a mixture of components in the system. The lower  $T_M$  can be assigned to p(TBS) (vide infra), and the higher  $T_M$  is consistent with PE.

Analysis of the  $^{13}\text{C}$  NMR spectrum of polymer produced in run 4 shows several striking differences compared with that of the 11 mol % ethene-*co*-TBS produced with 2/MAO.

Figure 3a shows the  $^{13}\text{C}$  NMR spectrum of high molecular weight, syndiotactic P(TBS) produced using  $\text{CpTiCl}_3/\text{MAO}$  in our laboratory. The  $\text{S}\alpha\alpha$  and  $\text{T}\beta\beta$  peaks (at 43.6 and 40.0 ppm, respectively) are sharp and solitary, indicating a highly stereo-

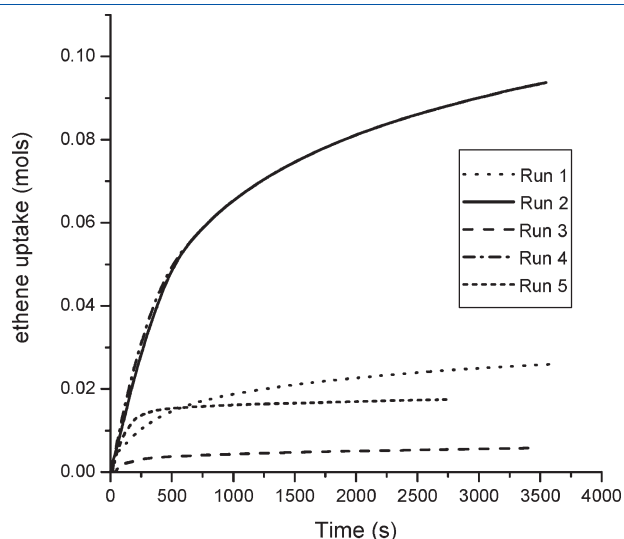


Figure 2. Ethene uptake profiles for runs 1–5.

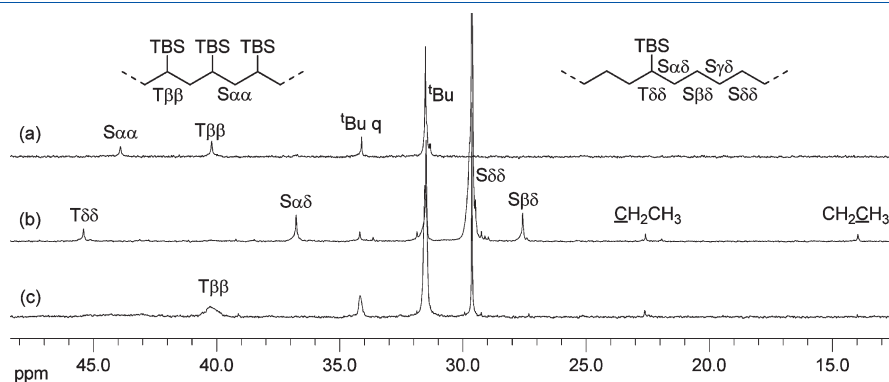


Figure 3.  $^{13}\text{C}$  NMR spectra of P(TBS) produced by (a)  $\text{CpTiCl}_3$ , (b) ethene-*co*-TBS produced with 2/MAO,<sup>34</sup> and (c)  $2/\text{Al}^i\text{Bu}_3/[\text{Ph}_3\text{C}][\text{B}(\text{C}_6\text{F}_5)_4]$  (run 2), with assignments.<sup>19,21,39,40</sup>

regular polymer. Figure 3b shows the spectrum of ethene-*co*-TBS produced by 2/MAO, indicating isolated TBS units ( $\text{T}\delta\delta$ ,  $\text{S}\alpha\delta$ ,  $\text{S}\alpha\gamma$ , and  $\text{S}\beta\delta$  at 45.0, 36.5, and 27.5 ppm, respectively). Also visible are the peaks associated with a terminal  $\text{CH}_3$  from PE (14.0 ppm) and the  $\text{CH}_2$  adjacent to this (22.3 ppm). Figure 3c is the spectrum of polymer formed with 2/ $\text{Al}^i\text{Bu}_3/[\text{Ph}_3\text{C}][\text{B}(\text{C}_6\text{F}_5)_4]$  (run 4). Here the  $\text{T}\delta\delta$  peak is not present. Instead, we see the  $\text{T}\beta\beta$  peak at 40.0 ppm, indicative of sequential TBS units. Unlike Figure 3a, this peak is broad and its associated  $\text{S}\alpha\alpha$  peak at 43.1 ppm is lost almost entirely in the baseline, suggesting atactic polymer. The few remaining peaks are readily assigned as belonging to either from P(TBS) (31.5 and 34.2 ppm,  $^t\text{Bu}$  ( $\text{CH}_3$ )<sub>3</sub> and  $^t\text{Bu}$  quaternary carbon, respectively) or PE (29.5 ppm,  $\text{S}\delta\delta$ ). No peaks for ethene/TBS copolymers are observed.

Thus, a combination of NMR, DSC, and GPC data point toward the formation of a blend of PE and P(TBS). Evidently then, the catalyst formed from 2/MAO has very different selectivity to that formed from 2/ $\text{Al}^i\text{Bu}_3/[\text{Ph}_3\text{C}][\text{B}(\text{C}_6\text{F}_5)_4]$ .

In order to exclude the possibility that the PE contaminant was being produced by the system at low concentrations of TBS toward the end of the 1 h reaction period, run 4 was conducted for 10 min. Analysis of the crude product and the Soxhlet fractions by NMR and DSC indicated that the polymer composition was broadly similar to that of run 2.

Run 5 shows that styrene is inactive in this system in place of TBS; ethene uptake dropped rapidly to near zero, and only traces of polymer were obtained from the system. This result corresponds with previous observations that the relative rates of the various styrenic monomer insertions are strongly affected by the substituents on the styrene ring, with alkylated styrenes favoring 1,2 insertion.<sup>25,26,41</sup> A number of further control experiments were carried out, and it was found that all three components (precatalyst **2**,  $\text{Al}^i\text{Bu}_3$ , and  $[\text{Ph}_3\text{C}][\text{B}(\text{C}_6\text{F}_5)_4]$ ) are required to furnish a catalytic system since removal of any one led to a complete loss of activity. Most interestingly, when the polymerization was repeated in the absence of ethene, very little polymer was produced (run 6). These results also exclude the possibility of a cationic/radical mechanism mediated by trityl or a Lewis acid-catalyzed process (via  $\text{Al}^i\text{Bu}_3$ ).

***tert*-Butylstyrene Homopolymerizations.** Given that ethene is required to produce a catalytic system, but that a homopolymer of TBS is the major mass product, we considered that ethene may be acting as a chain transfer agent (vide infra) and might be conveniently replaced by a monomer that would

Table 2. P(TBS) Polymerization Results with Catalyst 2<sup>a</sup>

run	cat. (mol)/10 <sup>-6</sup>	monomer system	yield (g)	mass prod <sup>b</sup>	TBS % conv	M <sub>n</sub>	PDI	T <sub>M</sub> (°C)
7	3.44	TBS/Hex	4.1	1192.0	76	3194	2.8	119.5
8	3.43	TBS/Hex	5.0	1453.7	87	4028	2.8	127.4
9	4.27	TBS/Hex	0.1	23.4	n/d	2284	1.8	
10	3.58	TBS/H <sub>2</sub> (g)	4.2	1174.1	77	4357	3.2	124.5
11	5.50	TBS/D <sub>2</sub> (g)	5.1	926.7	87	4977	2.6	137.1
12	3.71	TBS/Et <sub>3</sub> SiH	0.2	53.9	n/d	n/d	n/d	n/d
13	3.34	TBS/Pent	1.1	329.3	21	3320	2.5	121.1
14	2.98	TBS/St	7.3	2447.5	95	2556	3.2	104.0
15	3.03	TBS/DVB	6.3	2079.0	92	n/d	n/d	140.5

<sup>a</sup> Conditions: [Ph<sub>3</sub>C][B(C<sub>6</sub>F<sub>5</sub>)<sub>4</sub>] = 1.1 equiv to Zr; Al<sup>i</sup>Bu<sub>3</sub> = 100 equiv to Zr; ethene at 1.2 bar; [TBS] = 0.07 M; volume = 50 mL; run time = 60 min; T = 40 °C. <sup>b</sup> In kg-polymer/(mol-catalyst h).

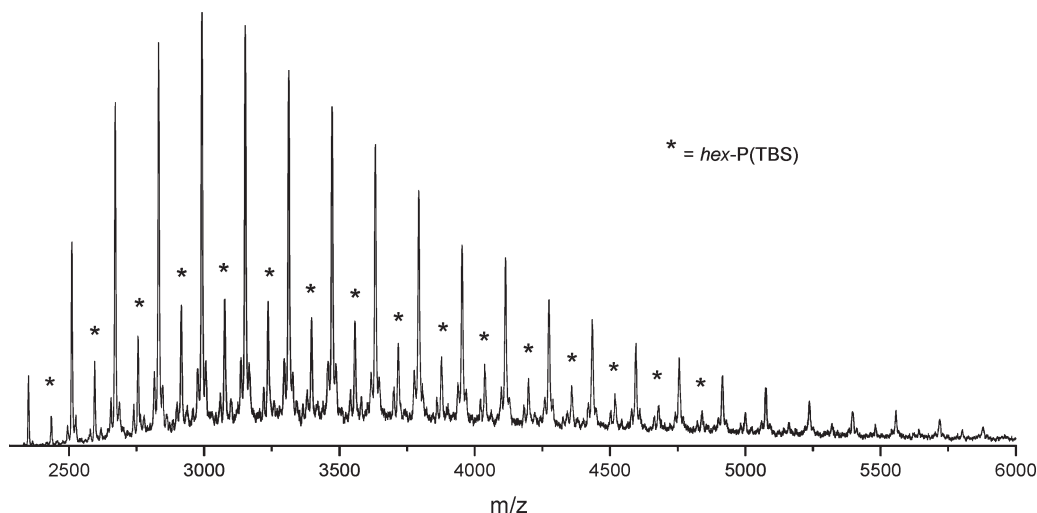


Figure 4. MALDI spectra of polymer obtained from run 7.

not itself also be homopolymerized in this system. We selected 1-hexene for this purpose, given that only titanium salicylaldimine systems activated with Al<sup>i</sup>Bu<sub>3</sub>/[Ph<sub>3</sub>C][B(C<sub>6</sub>F<sub>5</sub>)<sub>4</sub>] had been shown to homopolymerize this monomer.<sup>42</sup>

Run 7 (Table 2) shows the effect of adding 1-hexene to a TBS homopolymerization by 2/Al<sup>i</sup>Bu<sub>3</sub>/[Ph<sub>3</sub>C][B(C<sub>6</sub>F<sub>5</sub>)<sub>4</sub>]. After 1 h at 40 °C, 76% of the TBS had been converted. <sup>1</sup>H NMR suggested that P(TBS) had been formed exclusively. MALDI mass spectrometry (Figure 4) however showed two polymers: (i) P(TBS) with peaks spaced 160 Da apart as expected and (ii) P(TBS) with mass corresponding to a *single* unit of hexene having been incorporated—peaks spaced 160 Da apart but offset from P(TBS) by 84 Da (mass of hexene). On the basis of the masses observed, all polymers observed contain one in-chain double bond (vide infra).

Lowering the concentration of 1-hexene in the system (run 8, 0.1 equiv to TBS) gave P(TBS) only (within the detection limits of the MALDI experiment). Increasing the concentration of hexene (run 9, 10 equiv to TBS) lowered both the yield and the DoP but increased the proportion of hexene-terminated chains. Figure 5 shows MALDI spectra of both run 7 and run 9. In the spectra of run 7 the intensities of the peaks attributed to *hex*-P(TBS) are lower than those of P(TBS). In the spectra of run 9, this is reversed.<sup>43</sup>

Evidently then, hexene is in some way involved with the production of catalytic centers, i.e., as a promoter rather than a

conventional comonomer. As we have described above, benzylic dormant species are prevalent in E/S copolymerizations, and Chung has exploited this in the production of *p*-methylstyrene-terminated PE simply by addition of dihydrogen.<sup>44</sup> This produces an alkyl-terminated polymer and regenerates the catalyst by the mechanism shown in Figure 6. We were thus pleased to find that under 1 atm of H<sub>2</sub>, with no additional olefin “promoter”, P(TBS) was formed (run 10, Table 2). This run gave 4.2 g of free-flowing polymer and a conversion of 80% after 1 h, but interestingly we were unable to detect a loss of partial pressure of H<sub>2</sub> during the run.

GPC showed also that despite the presence of dihydrogen the homopolymer produced was very similar in M<sub>w</sub> to that produced above using hexene as a promoter. <sup>13</sup>C NMR spectra also show olefinic end groups (vide infra). Replacing H<sub>2</sub> with D<sub>2</sub> gave a yield of 5.1 g of polymer (run 11), comparable to that obtained in runs 7, 8, and 10. The MALDI spectra of P(TBS) from runs 10 and 11 indicated only vinyl-terminated polymer with no detectable incorporation of deuterium.

The use of silanes in olefin polymerization has been previously shown to produce end-capped PE and PS with both lanthanide and group IV transition metal catalysts.<sup>45,46</sup> Run 12 used triethylsilane in place of hexene/H<sub>2</sub>/D<sub>2</sub>. In accordance with previous results,<sup>47</sup> a significantly lower productivity rate was recorded than with either hexene, H<sub>2</sub>, or D<sub>2</sub>; however, Et<sub>3</sub>Si was incorporated onto the end of some P(TBS) chains. MALDI

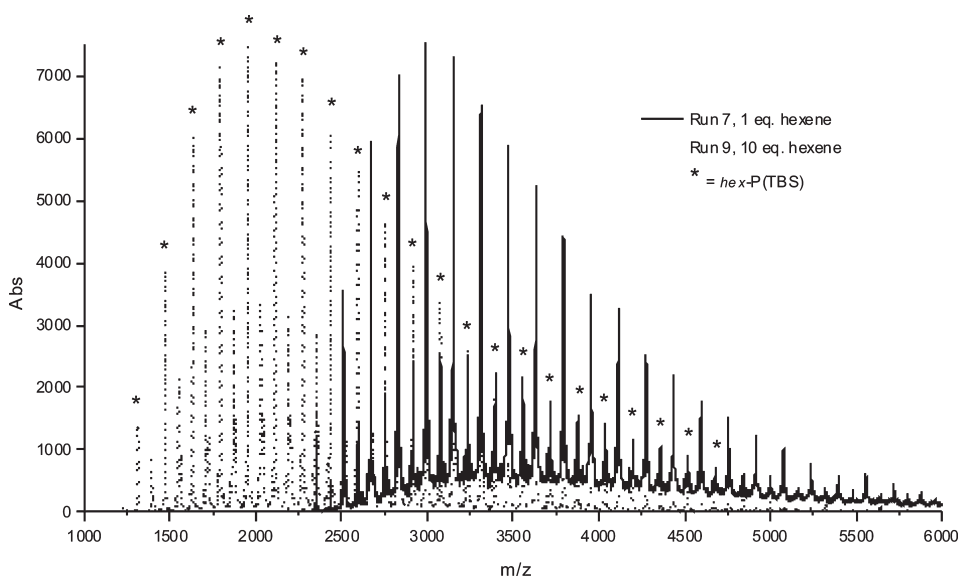


Figure 5. MALDI spectra of polymer obtained from runs 7 and 9.

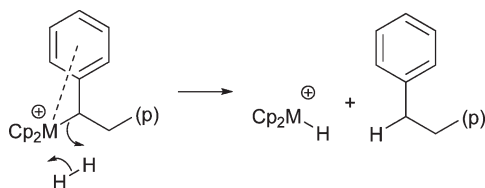


Figure 6. Chain transfer to  $H_2$  exemplified in the Chung system.<sup>44</sup>

of the resulting polymer shows two sets of peaks as with TBS/hexene, with an offset of 115 Da from each other (Figure 7).  $^1H$  NMR shows no ethyl peaks, indicating that incorporation of  $Et_3SiH$  is low. Polymerizations were also undertaken with vinyltrimethylsilane and diphenylsilane, though neither allowed the formation of P(TBS).

In an attempt to exploit the single monomer addition for use in postpolymerization functionalization reactions, copolymerizations with several hexene monomers were run: 5-hexenyl acetate, 5-hexen-2-one, 6-bromo-1-hexene, and 1,5-hexadiene. Of these, only the 1,5-hexadiene/TBS copolymerization yielded polymer (ca. 1.5 g). MALDI of this sample showed only peaks corresponding to P(TBS); i.e., no hexadiene addition was seen.

Further comonomers tried included 1-pentene, 1-heptene, 1-octene, 1-dodecene, divinylbenzene (DVB), and styrene. Unexpectedly, neither heptene, octene, nor dodecene showed addition to the P(TBS) formed, which was of low yield. Pentene fared better (run 13), producing 1.1 g of polymer, though MALDI suggested that there were fewer pentene-terminated chains than hexene-terminated chains under the same conditions. Polymerization of styrene/TBS was surprisingly successful (run 14), forming P(TBS) with ca. 18 mol % styrene incorporated according to  $^1H$  NMR spectra. This was confirmed by MALDI which showed P(TBS) chains with 1–3 styrene units each. Run 15 used 2 mol % DVB/TBS with which P(TBS) was formed in good yield, but without DVB addition according to MALDI. The high  $T_M$  for this run thus suggests a higher  $M_n$ , similar to that of 11, rather than cross-linking due to DVB.

The melting points shown for runs 7, 8, 10, and 11 generally increase with increased  $M_n$ . This may suggest that the p(TBS)

formed in the presence of ethene (vide supra) was of lower molecular weight than those formed in the presence of hexene or  $H_2$ .

**Mechanism.** We will begin by proposing a mechanism to account for our observations of the TBS homopolymerization by  $2/Al^iBu_3/[Ph_3C][B(C_6F_5)_4]$  in the presence of  $H_2$  (Scheme 2).

Cationic species **A** containing a polymeryl group (p) and coordinated TBS undergoes 1,2-insertion ( $a_{1,2}$ ) to give **B** which may either add further TBS to regenerate **A** or may, given the presence of a free coordination site at the metal, undergo  $\beta$ -elimination to give the 2-styrenyl-terminated polymer P(TBS)-2-sty. **A** may also undergo 2,1-insertion ( $a_{2,1}$ ) to give benzylic species **C**. This species is unlikely to undergo  $\beta$ -elimination or insertion since it does not have a suitable free coordination site for either of these processes (a dormant state; vide supra). Coordination of the arene as shown also orients the  $\beta$ -hydrogen atoms so that they may not coordinate to the metal to form the necessary transition state. Nevertheless,  $H_2$  (or  $D_2$ ) can regenerate the catalytic species through hydrogenolysis of the dormant state **C** (step c), releasing a P(TBS) chain. The coproduct from step c, hydride **D**, adds and inserts TBS (**d**) to regenerate **A**.

Without  $H_2$  (run 6) ca. 100 mg of polymer is produced before the catalyst becomes dormant or otherwise inactive. This equates to several polymer chains being produced through  $b_{\beta H}$ , i.e., the rate of  $b_{\beta H} \gg a_{2,1}$ , making P(TBS)-2-sty the major product, and P(TBS)-2H the minor. End-group analysis of the  $^{13}C$  NMR spectra (see Supporting Information) shows minor peaks at 111.5 and 145.3 ppm ( $CH_2$  and  $CCH_2$ , respectively), corresponding to polymer produced by  $b_{\beta H}$  (the major product). Alkyl peaks corresponding to the minor component P(TBS)-2H are not seen.

Our proposed mechanism for the hexene-cocatalyzed process (Scheme 3) is necessarily more complex. Species **A** undergoes propagation by 1,2-insertions of TBS ( $a_{1,2}$ ) with the possibility of termination by  $\beta$ -elimination ( $b_{\beta H}$ ) to give the observed P(TBS)-2-sty or 2,1 “mis-insertion” ( $a_{2,1}$ ) to give **C**, a “dormant state” as before. At step  $c_{BHT}$ , 1-hexene—which is not homopolymerized by this system (vide supra) but is rather less sterically demanding and more nucleophilic than TBS—approaches the dormant state and initiates a  $\beta$ -hydrogen transfer

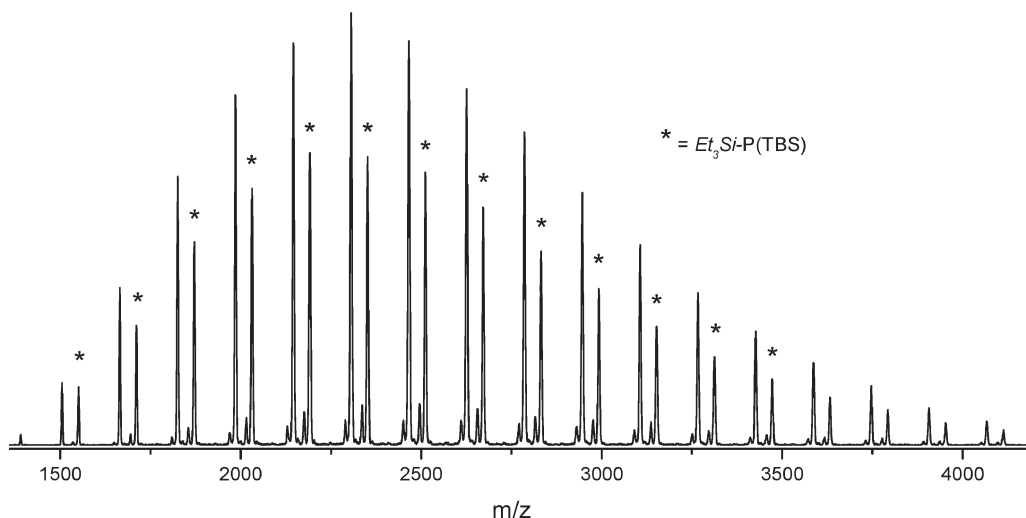
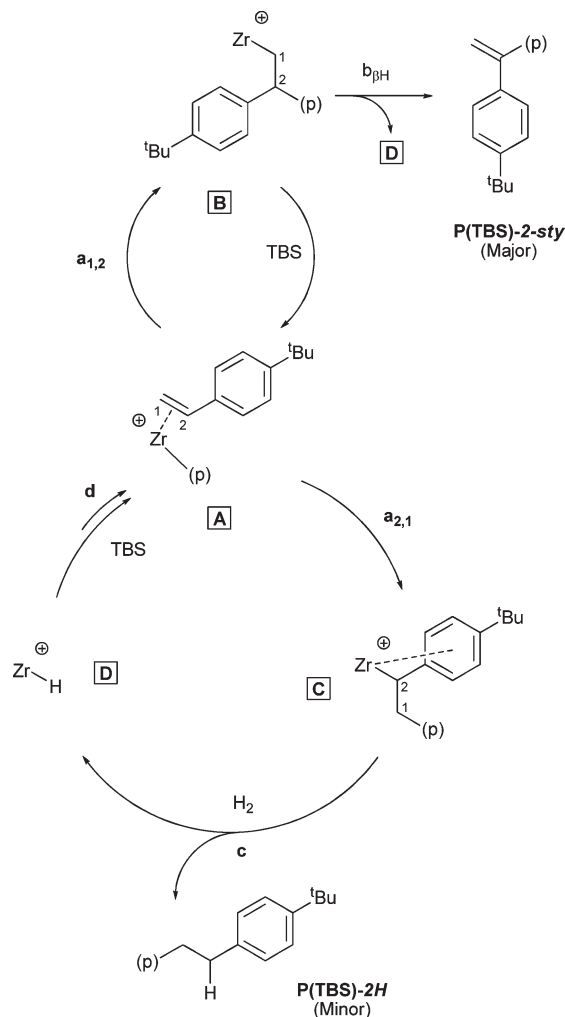


Figure 7. MALDI spectra of polymer obtained from run 12.

### Scheme 2. Proposed Mechanism of P(TBS) Formation Involving Chain Transfer to Dihydrogen



to monomer step. This releases the observed P(TBS)-1-sty and generates a hexyl species E.  $\beta$ -Hydride elimination at step  $e_{\beta H}$  releases 1-hexene and forms a metal hydride D.<sup>48</sup> This species

can then begin polymerization of TBS again via step d. Alternatively at E, a hexene-containing polymer chain is produced by addition and 1,2-insertion of TBS ( $e_{1,2}$ ) to give A'. This chain is subsequently propagated through B' via  $a'_{1,2}$ . TBS mis-insertion (step  $a'_{2,1}$ ) gives dormant state C' which, being resistant to  $\beta$ -elimination, undergoes  $\beta$ -hydride transfer to monomer as before ( $c'_{\beta H}$ ) to re-form E and eliminate hexyl-initiated and 1-styrenyl polymer *hex*-P(TBS)-1-sty.

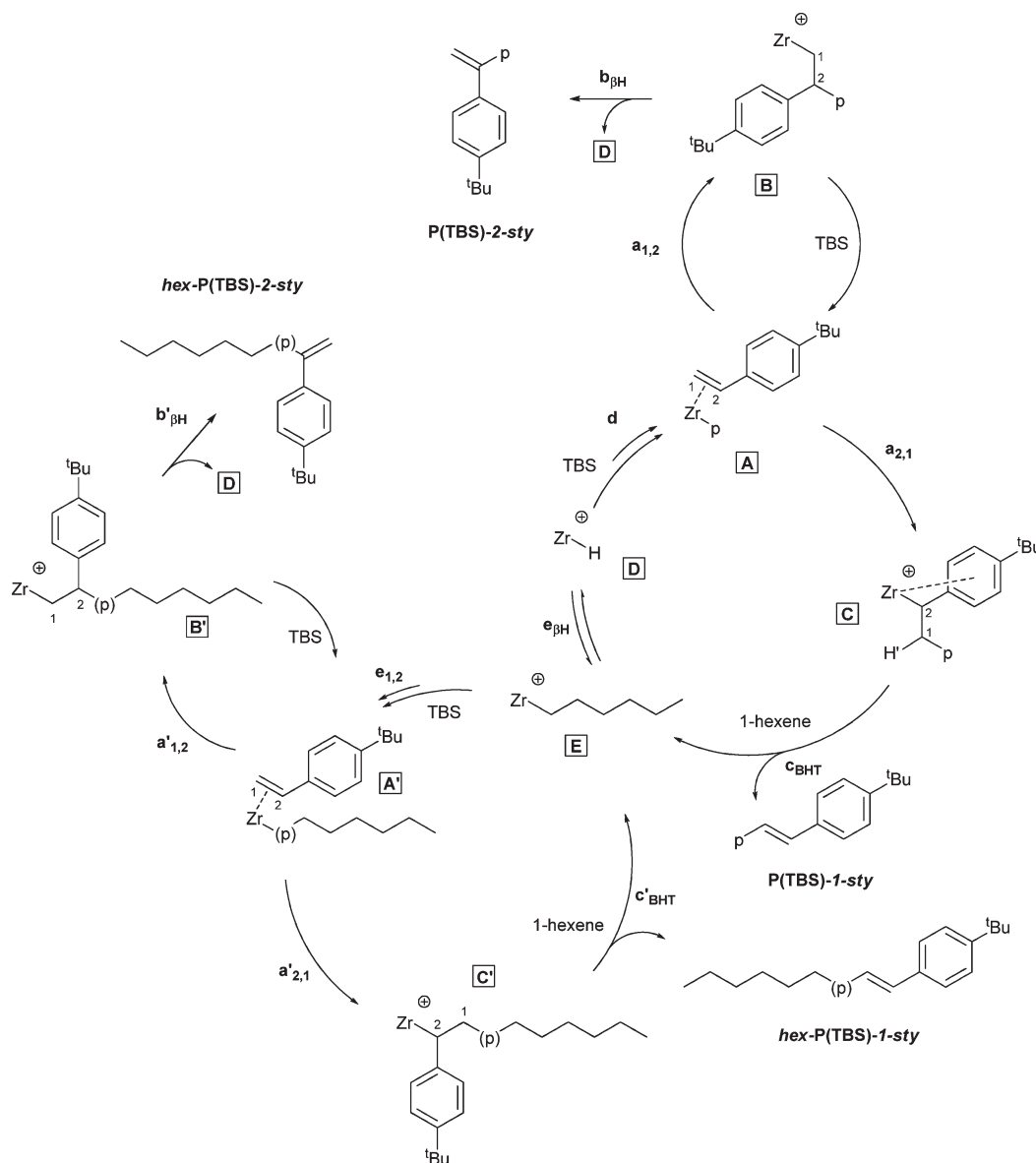
In this mechanism, the molecular weight of the -1-sty polymers is determined by the relative rates of  $a_{1,2}$  to  $a_{2,1}$  and  $a'_{1,2}$  to  $a'_{2,1}$ . Since species A and A' are identical in the region of the metal center following propagation, we would fully expect the rate constants for monomer insertions to be the same, i.e.,  $k(a_{1,2}) = k(a'_{1,2})$  and  $k(a_{2,1}) = k(a'_{2,1})$ . Hence, the observation of a similar molecular weight distribution, whether the chain contains hexene or not, is consistent with this mechanism. Similarly, the molecular weights of the -2-sty polymers are determined by the ratios of  $a_{1,2}$  to  $b_{\beta H}$  and  $a'_{1,2}$  to  $b'_{\beta H}$ ; again, as species B and B' are identical, molecular weights for -2-sty polymers will be the same. The ratio of hexyl- to non-hexyl-terminated polymer chains is determined by the relative rates of steps  $e_{\beta H}$  and  $e_{1,2}$ , with the rate of  $e_{\beta H} \gg e_{1,2}$  as indicated by the lack of resolvable hexyl peaks in either <sup>13</sup>C or <sup>1</sup>H NMR.

From the mechanism outlined in Scheme 3 we would expect a higher hexene concentration (cf. run 7 and run 9, 1, and 10 equiv of hexene, respectively) to produce significantly more hexyl-terminated polymer, and this was confirmed by MALDI spectrometry (Figure 5). Figure 8 shows GPC traces obtained for polymer from runs 7 and 9. The polymer from run 9 has a lower PDI (1.4) compared with that of run 7 (2.8), and the main peak corresponds to a shoulder of run 7. It is thus tentatively suggested that the major peak in run 7 is that of P(TBS)-2H while the major peak in run 9 is that of *hex*-P(TBS).

It is worth noting that salicylaldimine catalysts/MAO give multimodal GPC traces for PE. This has been attributed to multiple catalytic isomers present in the reaction,<sup>49–51</sup> though our catalyst studies suggest this is not the case here (vide infra). We also note our previous work showed that ethene/TBS copolymers produced with 2/MAO were formed by a single site mechanism, with a PDI of 2.<sup>34</sup>

We also note that the dominant 1,2 propagation steps in these mechanisms is likely to lead to atactic or syndio-rich polymer.

Scheme 3. Mechanism Outline of Chain Transfer to Monomer Providing P(TBS) with and without Hexene Termination



NMR spectra of the products are consistent with the former, suggesting a sterically unencumbered catalytic site (vide infra). In Figure 9 we have plotted  $T_M$  versus  $M_n$  for authentic homopolymers described in this work.  $T_M$  appears to reach a plateau well below the melting points of syndiotactic and isotactic p(TBS) (310 and 308 °C, respectively).<sup>8</sup>

**Catalyst Modifications.** After our initial success with runs 7 and 10, TBS/ $H_2$  homopolymerizations with catalysts **1** and **3** were initially undertaken alongside catalyst **2** (runs 16 and 17, Table 3). While no polymer precipitated in methanol as with run 10, organic work-up (DCM/1 M HCl<sub>(aq)</sub>) yielded several grams of low weight P(TBS). The melting points for these two polymers are also noticeably lower than run 10. This suggests the OMe group *para* to the O–Zr is important for formation of higher polymers either through a direct interaction with the cocatalyst or through its electron donation into the phenyl ring. To probe this, we synthesized zirconium dichloride precatalysts based on **4** and **5** (Figure 1) (runs 18–23, Table 3). Precatalyst **4**

( $L^4_2ZrCl_2$ ) was synthesized with a methoxy group *para* to the imine nitrogen. The molecular structure was determined by X-ray diffraction (Figure 10). The asymmetric unit contains half a complex composed of a phenoxyimine ligand and a chloride ligand attached to half a Zr atom which lies on a 2-fold axis. The angle between mean planes through the methoxyphenyl group and the chelate ring is 49.69(4)°. The angle between mean planes through the two chelate rings is 61.05(3)°. There is some possible  $\pi$  stacking between methoxy arene and phenoxide with closest C–C contact of 3.3237(23) Å and centroid–centroid distance of ca. 3.78 Å, but the angle between least-squares planes of these rings is rather high at ca. 20.9°. Nevertheless, there does not seem to be any steric reason why the rather “flattened” structure as shown in Figure 10 is adopted, with N(1)–Zr–N(1') of 72.17(6) Å and corresponding Cl(1)–Zr(1)–Cl(1') of 100.95(2).

Perhaps as a result of this unusual structure, this catalyst was found to give only a modest yield of ethene homopolymer



(run 18).  $^{13}\text{C}$  NMR spectra of the polymer produced using **4** in the ethene/TBS run 19 showed the sample to have a low incorporation of TBS (ca. 5%) with isolated TBS units. Correspondingly, this catalyst did not homopolymerize TBS under  $\text{H}_2$  (run 20).

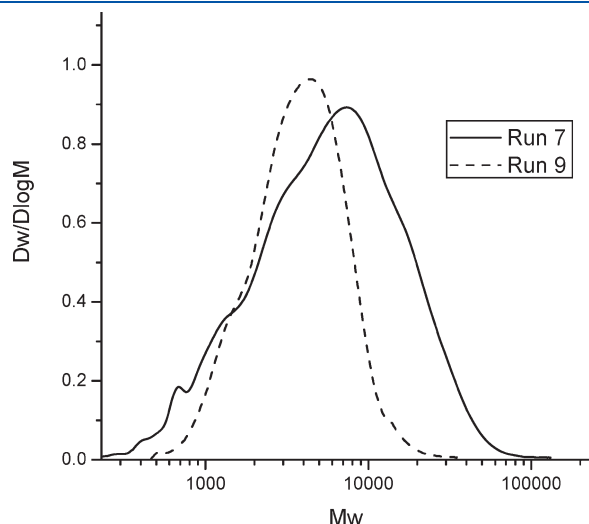


Figure 8. GPC spectra of selected polymers.

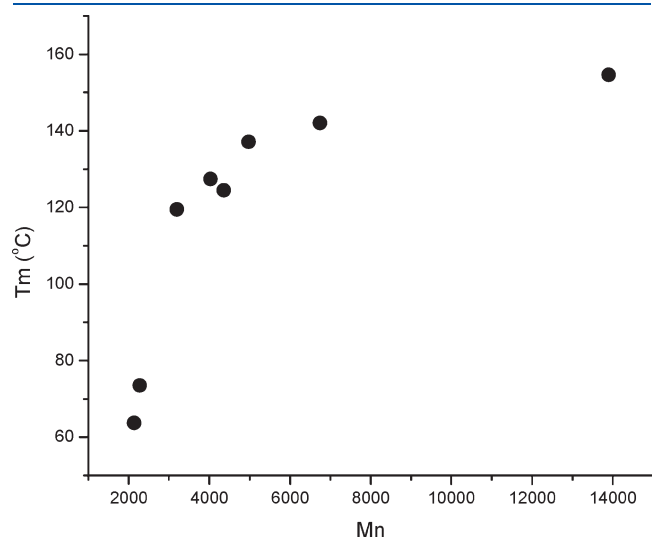


Figure 9.  $T_M$  vs  $M_n$  for selected TBS polymers.

Precatalyst **5** ( $\text{L}^5\text{ZrCl}_2$ ) was synthesized with a *tert*-butyl group *para* to the O–Zr unit. This catalyst system gives low yields of PE (run 21). Interestingly, while TBS/ $\text{H}_2$  homopolymerization produced only traces of polymer with this catalyst (run 23), TBS/ethene copolymerization produced P(TBS) (ca. 46% conversion) and traces of PE (run 22).

**Nature of the Catalytic Site.** Previous work on salicylaldimine systems has shown that replacing MAO with a combination of  $\text{Al}^i\text{Bu}_3/[\text{Ph}_3\text{C}][\text{B}(\text{C}_6\text{F}_5)_4]$  can have profound effects on the polymers produced. Zirconium salicylaldimine catalysts activated with MAO produce low-weight PE, whereas when activated with  $\text{Al}^i\text{Bu}_3/[\text{Ph}_3\text{C}][\text{B}(\text{C}_6\text{F}_5)_4]$  high-molecular-weight PE is formed.<sup>53</sup> This catalyst system also produces polypropylene (PP), unlike its MAO equivalent. Many of these changes are thought to be due not to the presence of a  $[\text{B}(\text{C}_6\text{F}_5)_4]^-$  counterion, but to the effect of aluminum alkyls on the precatalyst. Reduction of salicylaldimines to their corresponding amines has been shown to occur in situ upon addition of

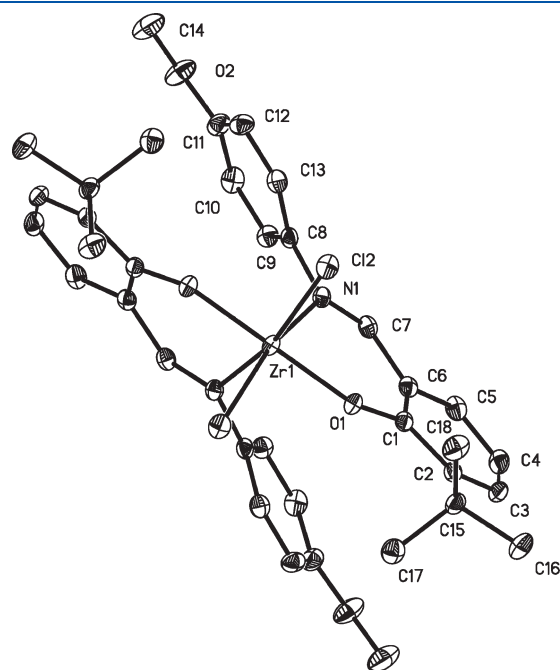


Figure 10. Molecular structure of **4** (H atoms omitted). Thermal ellipsoids shown at 50% probability. Selected bond lengths (Å) and angles (deg): Zr(1)–O(1) 1.9902(10), Zr(1)–N(1) 2.3480(13), Zr(1)–Cl(2) 2.4325(4), O(1)–Zr(1)–O(1') 167.59(6), N(1)–Zr(1)–N(1') 72.17(6), Cl(2)–Zr(1)–Cl(2') 100.95(2).

Table 3. Polymerizations with Functional Group-Modified Catalysts<sup>a</sup>

run	cat.	cat. (mol)/10 <sup>−6</sup>	monomer system	yield (g)	mass prod <sup>b</sup>	TBS % conv	$M_n$	PDI	$T_M$ (°C)
16	1	3.30	TBS/ $\text{H}_2(\text{g})$	2.1	636.0	36	2139	1.9	63.7
17	3	5.83	TBS/ $\text{H}_2(\text{g})$	3.4	950.5	56	2276	2.0	73.5
18	4	7.02	ethene	1.5	213.8	n/a			120.8
19	4	6.88	E/TBS	3.6	523.3	5			91.3
20	4	4.27	TBS/ $\text{H}_2(\text{g})$	0.0	0.0	n/a			
21	5	7.86	ethene	1.5	190.9	n/a			114.9
22	5	6.44	E/TBS	4.7	729.7	46			88.9, 123.6
23	5	4.64	TBS/ $\text{H}_2(\text{g})$	0.4	86.3	n/d			

<sup>a</sup> Conditions:  $[\text{Ph}_3\text{C}][\text{B}(\text{C}_6\text{F}_5)_4] = 1.1$  equiv to Zr;  $\text{Al}^i\text{Bu}_3 = 100$  equiv to Zr; ethene at 1.2 bar;  $[\text{TBS}] = 0.07$  M; volume = 100 mL (runs 18, 19, 21, and 22) or 50 mL (runs 16, 17, 20, and 23); run time = 60 min.;  $T = 40$  °C. <sup>b</sup> In kg-polymer/(mol-catalyst h).

Table 4. Polymerizations with Salicyloxazoline- and Salicylamine-Based Catalysts<sup>a</sup>

run	cat.	cat. (mol)/10 <sup>-6</sup>	monomer system	yield (g)	mass prod <sup>b</sup>	TBS % conv	<i>M</i> <sub>n</sub>	PDI	<i>T</i> <sub>M</sub> (°C)
24	2	4.68	E/TBS	2.2	469.8	40	n/d	n/d	127.3, 152.6
25	6	6.85	ethene	3.9	568.9	n/a	n/d	n/d	128.5
26	6	7.13	E/TBS	3.0	420.5	3	n/d	n/d	126.6
27	6	3.50	TBS/H <sub>2</sub> (g)	0.0	0.0	n/a	n/d	n/d	n/d
28	7	9.01	ethene	0.3	33.3	n/a	n/d	n/d	n/d
29	7	5.22	E/TBS	0.0	1.9	n/a	n/d	n/d	n/d
30	7	4.68	TBS/H <sub>2</sub> (g)	4.6	982.2	82	13 899	1.6	154.6
31	7	5.04	TBS/Hex	2.3	483.8	41	6745	2.1	142.0

<sup>a</sup> Conditions: [Ph<sub>3</sub>C][B(C<sub>6</sub>F<sub>5</sub>)<sub>4</sub>] = 1.1 equiv to Zr; Al<sup>i</sup>Bu<sub>3</sub> = 100 equiv to Zr; ethene at 1.2 bar; [TBS] = 0.07 M; volume = 100 mL (runs 24–26, 28, and 29) or 50 mL (runs 27, 30, and 31); run time = 60 min; *T* = 40 °C. <sup>b</sup> In kg-polymer/(mol-catalyst h).

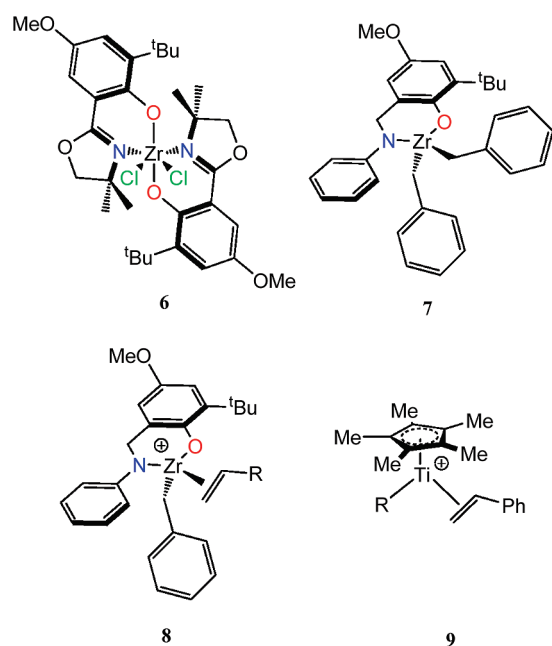


Figure 11. Salicyloxazoline and salicylamido complexes.

Al<sup>i</sup>Bu<sub>3</sub> or in the case of metal dibenzyl species through a 1,2 migratory insertion of a benzyl group from the metal center.<sup>54,55</sup> Furthermore, Pellecchia and co-workers have synthesized complementary salen(imine) and salen(amine) complexes. When activated with Al<sup>i</sup>Bu<sub>3</sub> and MAO, respectively, these systems gave comparable results for polymerization of several different monomers.<sup>56</sup>

Our investigation into this phenomenon and the nature of the active site in our Zr system began with run 24 (Table 4). Catalyst 2 was premixed with 5 equiv of Al<sup>i</sup>Bu<sub>3</sub> in toluene for 30 min prior to injection into the reaction vessel to allow any imine reduction to take place. Although the yield of P(TBS) was relatively low, no ethene uptake was seen, and no evidence of PE was found by NMR spectroscopy. This result indicates that while a catalyst for PE synthesis is produced on first activation of 2, this converts to a catalyst for production of P(TBS). This is of course consistent with the results in Table 1.

Our bis-salicyloxazoline group 4 complexes have been shown to be resistant to reduction and when activated with either MAO or borates are capable of very high activity polymerization of olefins.<sup>36,57</sup> The salicyloxazoline catalyst 6 (L<sup>6</sup><sub>2</sub>ZrCl<sub>2</sub>) (Figure 11) polymerized ethene in the presence of Al<sup>i</sup>Bu<sub>3</sub>/[Ph<sub>3</sub>C][B(C<sub>6</sub>F<sub>5</sub>)<sub>4</sub>] (run 25), while in the presence of

TBS (run 26) a copolymer was produced (ca. 3 mol % TBS, isolated TBS units by <sup>13</sup>C NMR and further suggested by the high *T*<sub>M</sub>). This latter behavior is the same as that of 2/MAO. Correspondingly, no polymer is formed during attempted TBS homopolymerization by 6/Al<sup>i</sup>Bu<sub>3</sub>/[Ph<sub>3</sub>C][B(C<sub>6</sub>F<sub>5</sub>)<sub>4</sub>] under an atmosphere of dihydrogen (run 27).

The above results are consistent with a reduced Schiff base catalyst system being produced from 2. We thus synthesized 7 (L<sup>7</sup>ZrBn<sub>2</sub>), a new member of a class of salicylamido zirconium compounds introduced by Gibson.<sup>38</sup> We first confirmed Gibson's reports<sup>38,58</sup> that the aluminum-free catalyst system 7/[Ph<sub>3</sub>C][B(C<sub>6</sub>F<sub>5</sub>)<sub>4</sub>] is inactive for PE (run 28, Table 4) and then showed that it is highly active for TBS polymerization in the presence of H<sub>2</sub> or hexene (runs 30 and 31, respectively).

Interestingly, P(TBS) is not formed in the presence of ethene (run 29). Productivities are comparable to those of 2/Al<sup>i</sup>Bu<sub>3</sub>/[Ph<sub>3</sub>C][B(C<sub>6</sub>F<sub>5</sub>)<sub>4</sub>] (compare runs 10/30 and 7/31), as are the molecular weight and PDI of the polymers produced.

## CONCLUSIONS

In the presence of Al<sup>i</sup>Bu<sub>3</sub>/[Ph<sub>3</sub>C][B(C<sub>6</sub>F<sub>5</sub>)<sub>4</sub>] the zirconium precatalysts 1–3 are converted to a catalytic species which act in essentially the same manner as the aluminum-free 7/[Ph<sub>3</sub>C][B(C<sub>6</sub>F<sub>5</sub>)<sub>4</sub>] system. The implication is that the catalyst in both cases is closely related to the propagating cationic species 8. The lack of activity in the absence of added aliphatic monomer or dihydrogen is accounted for by two related mechanisms. Hexene awakens a benzylic dormant state by a familiar β-hydrogen transfer to monomer (BHT) process,<sup>59,60</sup> and this leads to the observed products (some containing one hexene unit, and some none, plus two different unsaturated end groups). Dihydrogen takes part in a “chain transfer to hydrogen” mechanism, allowing catalyst regeneration (Scheme 2).

The catalytic activity in this system is finely balanced. For example, substituents on the catalyst affect the activity and *M*<sub>w</sub> of the polymer produced (cf. 2 with 1 and 3). Styrene itself is not polymerized, presumably because the benzylic dormant species formed by this unsubstituted monomer is more stable than its TBS analogue.<sup>34</sup> There is also a striking similarity in terms of functionality between 8 and the proposed active species 9 from Ishihara's classic sPS catalyst,<sup>3,4</sup> the chief difference between the two being that 9 produces syndiotactic PS due to the prevalence of the 2,1 insertion,<sup>3</sup> whereas in 8, 1,2 insertions lead to formation of atactic polymer.

These new catalytic systems for polymerization of TBS are exceptionally active considering the usual poor performance of

Zr compared with Ti for PS catalysis as reviewed above. The results indicate how we might in future be able to produce practical Zr catalysts for PS catalysis; it may be that many known poorly active (or perhaps dormant) systems could be awakened using dihydrogen or alkenes as chain transfer agents.

## ■ ASSOCIATED CONTENT

**S Supporting Information.**  $^{13}\text{C}$  spectra of p(TBS) and crystallographic data for complex 4 in .cif format. This material is available free of charge via the Internet at <http://pubs.acs.org>.

## ■ AUTHOR INFORMATION

### Corresponding Author

\*E-mail: Peter.Scott@warwick.ac.uk.

## ■ ACKNOWLEDGMENT

An Oxford Diffraction Gemini XRD system and polymer characterization equipment were obtained through the Science City Advanced Materials project 1 and 2, respectively, with support from Advantage West Midlands (AWM) and part funded by the European Regional Development Fund (ERDF). We thank EPSRC and Infineum for funding through a Warwick Collaborative Training Account and Warwick Knowledge Transfer Secondments (G.W.T.).

## ■ REFERENCES

- (1) Schellenberg, J.; Tomotsu, N. *Prog. Polym. Sci.* **2002**, 27 (9), 1925–1982.
- (2) Rodrigues, A. S.; Kirillov, E.; Carpentier, J. F. *Coord. Chem. Rev.* **2008**, 252 (18–20), 2115–2136.
- (3) Ishihara, N.; Seimiya, T.; Kuramoto, M.; Uoi, M. *Macromolecules* **1986**, 19 (9), 2464–2465.
- (4) Ishihara, N.; Kuramoto, M.; Uoi, M. *Macromolecules* **1988**, 21 (12), 3356–3360.
- (5) Grassi, A.; Pellecchia, C.; Longo, P.; Zambelli, A. *Gazz. Chim. Ital.* **1987**, 117 (4), 249–250.
- (6) Ishihara, N.; Kuramoto, M. In *Synthesis and Properties of Syndiotactic Polystyrene*; International Symposium on Catalyst Design for Tailor-Made Polyolefins, Kanazawa, Japan, Mar 10–12; Soga, K., Terano, M., Eds.; Kanazawa, Japan, 1994; pp 339–350.
- (7) Proto, A.; Luciano, E.; Capacchione, C.; Motta, O. *Macromol. Rapid Commun.* **2002**, 23 (3), 183–186.
- (8) Tomotsu, N.; Ishihara, N.; Newman, T. H.; Malanga, M. T. *J. Mol. Catal. A: Chem.* **1998**, 128 (1–3), 167–190.
- (9) Rahmani, S.; Abbasian, M.; Moghadam, P. N.; Entezami, A. A. *J. Appl. Polym. Sci.* **2007**, 104 (6), 4008–4014.
- (10) Caporaso, L.; Izzo, L.; Sisti, I.; Oliva, L. *Macromolecules* **2002**, 35 (13), 4866–4870.
- (11) Beckerle, K.; Capacchione, C.; Ebeling, H.; Manivannan, R.; Mulhaupt, R.; Proto, A.; Spaniol, T. P.; Okuda, J. *J. Organomet. Chem.* **2004**, 689 (24), 4636–4641.
- (12) Longo, P.; Grassi, A.; Oliva, L. *Makromol. Chem.* **1990**, 191 (10), 2387–2396.
- (13) Williams, E. F.; Murray, M. C.; Baird, M. C. *Macromolecules* **2000**, 33 (2), 261–268.
- (14) Po, R.; Cardi, N. *Prog. Polym. Sci.* **1996**, 21 (1), 47–88.
- (15) Chien, J. C. W.; Salajka, Z.; Dong, S. *Macromolecules* **1992**, 25 (12), 3199–3203.
- (16) Ready, T. E.; Gurge, R.; Chien, J. C. W.; Rausch, M. D. *Organometallics* **1998**, 17 (24), 5236–5239.
- (17) Grassi, A.; Zambelli, A.; Laschi, F. *Organometallics* **1996**, 15 (2), 480–482.
- (18) Chum, P. S.; Kruper, W. J.; Guest, M. J. *Adv. Mater.* **2000**, 12 (23), 1759–1767.
- (19) Arai, T.; Ohtsu, T.; Suzuki, S. *Macromol. Rapid Commun.* **1998**, 19 (6), 327–331.
- (20) Sernetz, F. G.; Mulhaupt, R.; Amor, F.; Eberle, T.; Okuda, J. *J. Polym. Sci., Part A: Polym. Chem.* **1997**, 35 (8), 1571–1578.
- (21) Sernetz, F. G.; Mulhaupt, R.; Waymouth, R. M. *Macromol. Chem. Phys.* **1996**, 197 (3), 1071–1083.
- (22) Arriola, D. J.; Bokota, M.; Campbell, R. E.; Klosin, J.; LaPointe, R. E.; Redwine, O. D.; Shankar, R. B.; Timmers, F. J.; Abboud, K. A. *J. Am. Chem. Soc.* **2007**, 129 (22), 7065–7076.
- (23) Chirik, P. J.; Bercaw, J. E. *Organometallics* **2005**, 24 (22), 5407–5423.
- (24) Naga, N.; Wakita, Y.; Murase, S. *J. Appl. Polym. Sci.* **2008**, 110 (6), 3770–3777.
- (25) Correa, A.; Galdi, N.; Izzo, L.; Cavallo, L.; Oliva, L. *Organometallics* **2008**, 27 (6), 1028–1029.
- (26) Theaker, G. W.; Morton, C.; Scott, P. *J. Polym. Sci., Part A: Polym. Chem.* **2009**, 47 (12), 3111–3117.
- (27) Matsui, S.; Mitani, M.; Saito, J.; Tohi, Y.; Makio, H.; Matsukawa, N.; Takagi, Y.; Tsuru, K.; Nitabar, M.; Nakano, T.; Tanaka, H.; Kashiwa, N.; Fujita, T. *J. Am. Chem. Soc.* **2001**, 123 (28), 6847–6856.
- (28) Matsui, S.; Mitani, M.; Saito, J.; Tohi, Y.; Makio, H.; Tanaka, H.; Fujita, T. *Chem. Lett.* **1999**, 12, 1263–1264.
- (29) Matsui, S.; Tohi, Y.; Mitani, M.; Saito, J.; Makio, H.; Tanaka, H.; Nitabar, M.; Nakano, T.; Fujita, T. *Chem. Lett.* **1999**, 10, 1065–1066.
- (30) Hustad, P. D.; Tian, J.; Coates, G. W. *J. Am. Chem. Soc.* **2002**, 124 (14), 3614–3621.
- (31) Tian, J.; Coates, G. W. *Angew. Chem., Int. Ed.* **2000**, 39 (20), 3626–3629.
- (32) Tian, J.; Hustad, P. D.; Coates, G. W. *J. Am. Chem. Soc.* **2001**, 123 (21), 5134–5135.
- (33) Weiser, M. S.; Mulhaupt, R. *Macromol. Rapid Commun.* **2006**, 27 (13), 1009–1014.
- (34) Theaker, G. W.; Morton, C.; Scott, P. *Dalton Trans.* **2008**, 48, 6883–6885.
- (35) Gottlieb, H. E.; Kotlyar, V.; Nudelman, A. *J. Org. Chem.* **1997**, 62 (21), 7512–7515.
- (36) Bott, R. K. J.; Hammond, M.; Horton, P. N.; Lancaster, S. J.; Bochmann, M.; Scott, P. *Dalton Trans.* **2005**, 22, 3611–3613.
- (37) Scott, P. Alkylation of zirconium tetrachloride with benzyl Grignard. <http://cssp.chemspider.com/1> <http://dx.doi.org/10.1039/SP1>.
- (38) Oakes, D. C. H.; Kimberley, B. S.; Gibson, V. C.; Jones, D. J.; White, A. J. P.; Williams, D. J. *Chem. Commun.* **2004**, 19, 2174–2175.
- (39) Martinez, S.; Exposito, M. T.; Ramos, J.; Cruz, V.; Martinez, M. C.; Lopez, M.; Munoz-Escalona, A.; Martinez-Salazar, J. *J. Polym. Sci., Part A: Polym. Chem.* **2005**, 43 (4), 711–725.
- (40) Nomura, K.; Okumura, H.; Komatsu, T.; Naga, N.; Imanishi, Y. *J. Mol. Catal. A: Chem.* **2002**, 190 (1–2), 225–234.
- (41) Chung, T. C.; Lu, H. L. *J. Polym. Sci., Part A: Polym. Chem.* **1998**, 36 (6), 1017–1029.
- (42) We have confirmed this experimentally in the current system.
- (43) We note that the  $M_n$  apparent in the MALDI spectra (ca. 3000 for run 7) is substantially lower than that obtained by GPC (ca. 7000 for the same run).
- (44) Dong, J. Y.; Chung, T. C. *Macromolecules* **2002**, 35 (5), 1622–1631.
- (45) Koo, K. M.; Marks, T. J. *J. Am. Chem. Soc.* **1998**, 120 (16), 4019–4020.
- (46) Koo, K.; Marks, T. J. *J. Am. Chem. Soc.* **1999**, 121 (38), 8791–8802.
- (47) Makio, H.; Koo, K.; Marks, T. J. *Macromolecules* **2001**, 34 (14), 4676–4679.
- (48) Although no polyhexene is formed from this system, hexene coordination may occur, rendering this step reversible.
- (49) Haruyuki Makio, T. F. *Macromol. Symp.* **2004**, 213 (1), 221–234.

- (50) Sanz, M.; Cuenca, T.; Cuomo, C.; Grassi, A. J. *Organomet. Chem.* **2006**, 691 (18), 3816–3822.
- (51) Tohi, Y.; Makio, H.; Matsui, S.; Onda, M.; Fujita, T. *Macromolecules* **2003**, 36 (3), 523–525.
- (52) Janiak, C. *Dalton Trans.* **2000**, 21, 3885–3896.
- (53) Makio, H.; Kashiwa, N.; Fujita, T. *Adv. Synth. Catal.* **2002**, 344 (5), 477–493.
- (54) Knight, P. D.; O'Shaughnessy, P. N.; Munslow, I. J.; Kimberley, B. S.; Scott, P. J. *Organomet. Chem.* **2003**, 683 (1), 103–113.
- (55) Knight, P. D.; Clarkson, G.; Hammond, M. L.; Kimberley, B. S.; Scott, P. J. *Organomet. Chem.* **2005**, 690 (23), 5125–5144.
- (56) Strianese, M.; Lambert, M.; Mazzeo, M.; Pellicchia, C. *Macromol. Chem. Phys.* **2008**, 209 (6), 585–592.
- (57) Coles, S. R.; Clarkson, G. J.; Gott, A. L.; Munslow, I. J.; Spitzmesser, S. K.; Scott, P. *Organometallics* **2006**, 25 (26), 6019–6029.
- (58) Cariou, R.; Gibson, V. C.; Tomov, A. K.; White, A. J. P. *J. Organomet. Chem.* **2009**, 694 (5), 703–716.
- (59) Talarico, G.; Budzelaar, P. H. M. *J. Am. Chem. Soc.* **2006**, 128 (14), 4524–4525.
- (60) Talarico, G.; Budzelaar, P. H. M. *Organometallics* **2008**, 27 (16), 4098–4107.